Electronic Structure of Metallic Glasses from the Cu-Zr- and Cu-Ti-Systems as well as from some Transitionmetall-Metalloid-Systems by Means of X-Ray-Emission Spectroscopy

Siegfried Falch, Georg Rainer-Harbach, Friedrich Schmückle, and Siegfried Steeb

Max-Planck-Institut für Metallforschung, Institut für Werkstoffwissenschaften, Stuttgart

Using an electron microprobe, the position and shape of the characteristic X-Ray emission lines from the elements Cu, Zr, Ti, Fe, Co, and Mn in metallic glasses of the systems Cu-Zr, Cu-Ti, Fe-B, Fe-P, Co-B, Co-P, Fe-Ge-P, Mn-Si-P, and Fe-Si-P were studied. In each case the lines were compared with those of either the crystalline element or the corresponding crystalline compound. Compared to electron spectroscopy methods such as XPS or UPS, the method used during this work has the advantage that the spectra obtained are specific for the corresponding element. The general trend of the results can be described in such a way that the energy of binding of the electrons to the corresponding atomic species is larger in the amorphous state than in the crystalline element, whereas the energy of binding of the electrons in the amorphous state is similar to that of the corresponding crystalline compound.

1. Introduction

There exists a number of empirical efforts with the aim to understand the conditions for glass-forming which led with some success to the evaluation of some rules. According to some theoretical work [1], [2], [3], the stabilizing of the amorphous phase depends very strongly from the electronic structures. The results of electron spectroscopical measurements [4], [5] point to a stabilization of the glasses by additional binding states. The methods used were γ-photoelectron spectroscopy (XPS) and UV-photoelectron spectroscopy (UPS). Thermo-dynamic investigations show a connection between exothermal heat of mixing and good glass forming ability [6]. Also structural investigations with Fe-B-, Cu-Zr- or Mn-Si-P-metallic glasses [7], [8] prove chemical short range order, i.e. stabilization of the molten alloy by compound formation and thus favourisation of glass formation. Up to now only very few investigations of the electronic structure were performed using X-Ray emission spectroscopy. By this method the specimen is excited for example within an electron microprobe by electrons and the position and shape of the emitted characteristic X-Ray line is measured.

Since the band structure within the metals and alloys is determined mainly by the component atoms and their arrangement, by the method of band spectroscopy one can obtain information about fundamental properties of the solid state. By electron spectroscopy the energy of binding as well of the core electrons as of the shell electrons can be determined. However, it is not possible to determine the partial density of states, i.e. the origin of the analyzed electrons. Furthermore there exist certain problems in the energy determination caused by charging the specimen [9], [10]. Contrary to electron spectroscopy, X-Ray emission spectroscopy yields information about the local partial densities of states of the valence bands [11], and thus represents an interesting method of investigation especially for binary systems. We have to pay attention to the fact, however, that the access to the density of states is not so direct as with electron spectroscopy.

By means of quantum mechanics one can learn that the shape of X-Ray emission spectra represents the density of states modulated by the transition probability. Assuming this transition probability to be constant referred to the valence band, a true picture of the local partial density of states within the valence band spectrum can be obtained [12]. For a precise analysis of the X-Ray emission all the factors must be taken into consideration which influence the transition. These are mainly the atomic arrangement and broadening effects caused by Auger transitions. Also distortions by the instrument, the influence of the acceleration

voltage and the absorption within the specimen should be mentioned [13], [14]. During the present work the fact is used [15], [16] that the X-Ray-spectra emitted by the atoms of a certain kind depend in their position as well as in their shape extremely from the chemical and topological surrounding of the corresponding atom. Especially the difference between the crystalline and the amorphous state will be treated.

2. Experimental Fundamentals

During the present work it was necessary to measure the L-spectra of single elements in metallic glasses and in crystalline phases of various systems. For these measurements an electron microprobe is especially convenient since such an instrument normally is capable to perform quantitative analytical work and therefore works sufficiently accurate. With the instrument JSM 50 A (Jeol, Tokyo) it was necessary for the elimination of carbon-contamination to use a turbo pump instead of a diffusion pump. Furthermore these measurements only could be done with a special software which controls the experimental runs and the data acquisition by means of a computer (pdp 11/05; DEC) via a corresponding electronic control system (Datanim; Canberra). This equipment enabled to run one after the other up to ten spectrometer scans with different specimens without manual contact.

The optimum adjustment of the specimen onto the Rowland circle was done in two steps. The first was the rough adjustment by means of an optical microscope. The second consisted in an automatical adjustment with the aid of the X-Ray spectrometer. During this process the specimen was shifted up and down within ± 0.02 mm around the "rough" position by steps of 0.001 mm until optimum X-Ray intensity was obtained.

The contamination of the specimen and the instabilities of the high voltage as well as of the beam current lead together with an eventual drift of the electronic equipment to long time variations of the intensity. To exclude these effects, the following procedure was followed: The intensity measured at each spectrometer position was related to the intensity obtained at the spectrometer position corresponding to the maximum. Thus for each point a relative intensity I_{rel} was obtained.

$$I_{\text{rel}} = \frac{I_\theta}{I_{\text{curr }1}} : \frac{I_{\text{max}}}{I_{\text{curr }2}}, \qquad (1)$$

I_θ intensity at the angle θ,

I_{max} intensity at the maximum,

I_{rel} relative intensity,

$I_{\text{curr }1}$ integrated beam current during measuring at the point θ,

$I_{\text{curr }2}$ integrated beam current during measuring at the maximum.

By this method it was possible to work without further beam stabilizing facilities up to beam currents of 10^{-7} A which allowed the measurement of weak lines with sufficient low statistical error. The accelerating voltage for the best peak to background ratio amounted to 15 kV for Zirconium and to 10 kV for the other elements.

Concerning the influence of self absorption on the shape of the emission line it should be mentioned, that this effect changes mainly the high-energy side of the emission line and to a smaller extent also the line position (see later). Since, however, during the measurements the accelerating voltage remained unchanged and since the take off angle of the spectrometer was from instrumental reasons constant, a correction of the effect of self absorption could be avoided.

The smoothing of the experimental curves was done according to the method of cubic spline fit. The smoothing was favorable in point of view of the desmearing. Otherwise the physical irrelevant statistical fluctuations would have been intensified too much by the mathematical desmearing process.

Since the experimental spectrum represents the convolution of the spectrum with the instrumental distribution [14], [17], the experimental spectrum must be desmeared to obtain the true spectrum. The instrumental distribution results from the entrance slit, the variations in the curvature of the crystal [14], the mosaic spread of the crystal, the deviation from the geometry (Rowland-circle), and the play of gears.

For the determination of the instrumental distribution the higher orders ($n = 2, 5, 6$) of the Ti-Lα-line were measured exactly and assumed that the measured line-width corresponds to the instrumental distribution. The software developed for the desmearing procedure [18] is mainly based on the References [17], [19].

3. Performance of the Experiments, Results and Discussion

Characteristic X-Ray emission lines were measured with metallic glasses of the following systems: Fe-B, Cu-Ti, Cu-Zr, Co-B, Co-P, Fe-P, Ni-P, Mn-Si-P, Fe-Si-B, and Fe-Ge-P.

The amorphous specimens were prepared as ribbons (breadth 2—4 mm, Thickness < 35 μm) within a melt-spin apparatus [20]. With all elements the $L\alpha_{1,2}$-line was obtained, to which within the atoms corresponds the transition from the 3d-(4d or 5d-) band, respectively, to the corresponding L_{III}-niveau. In case of Zirconium the $L\beta_{2,15}$-line was used. For the $L\alpha$-lines a RAP- and for the $L\beta_{2,15}$-line a PET-crystal was used. The spectra were obtained using a step width of 0.02 mm, corresponding to a wavelength step of about $1.9 \cdot 10^{-3}$ Å (RAP; Cu-Lα) or of about $6.2 \cdot 10^{-4}$ Å (PET, Zr-Lβ).

To reach maximum reproducibility, the play of the gears had to be kept low. Therefore all positions were approached with slowing down velocity and only from one direction.

a) Cu-Zr- and Cu-Ti-systems

The Figs. 1a and 1b show the Lα-spectra of copper in crystalline intermetallic Cu-Zr-compounds and in amorphous Cu-Zr-alloys. All curves show a bump in the energy region which corresponds to the energy of the absorption [21]. The maximum is shifted to lower energies with decreasing copper concentration, a shoulder or a peak being shaped at the same time.

The Figs. 2a and 2b show the $L\beta_{2,15}$-spectra of Zr within the same alloys. The absorption edge [21] lies at the right hand side border of the energy scale. No change can be observed in the position of the maxima compared to pure Zr within the concentration range of the amorphous phases. Only the crystalline $Cu_{50}Zr_{50}$-phase shows a slight shift of the maximum to higher energies. With increasing Cu-concentration a shoulder or a peak, respectively, is formed on the low energy side in a distance of 3 to 4 eV from the maximum.

The Figs. 3a and 3b show the Lα-spectra of copper in different crystalline Cu-Ti-phases and in two metallic glasses from the Cu-Ti-system compared to pure Cu. The Ti-Lα-line could not be measured because of its coincidence with the Cu-Lα-line of second order. Also in Figs. 3a and 3b the bump of
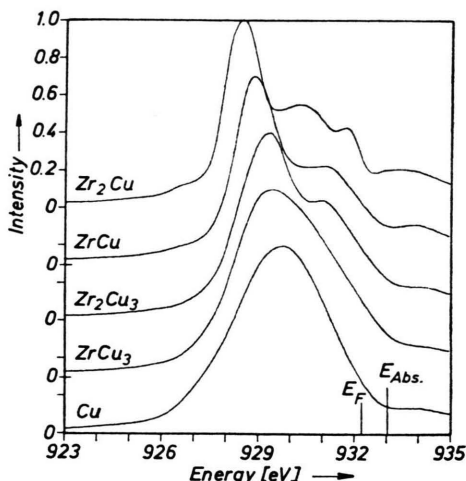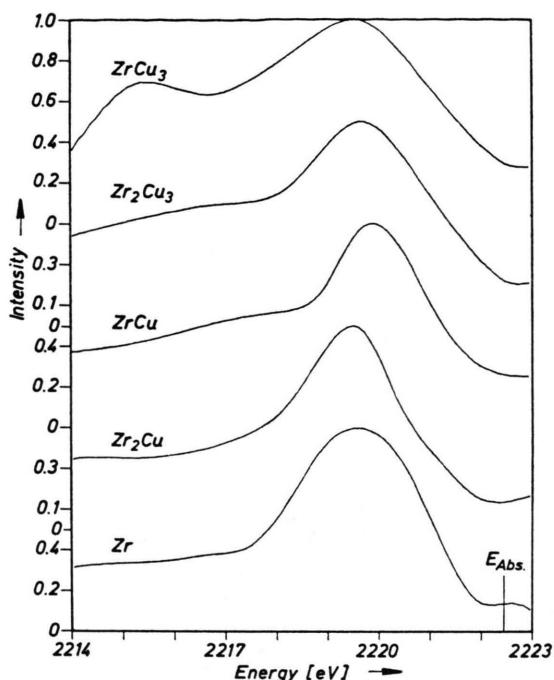

a)
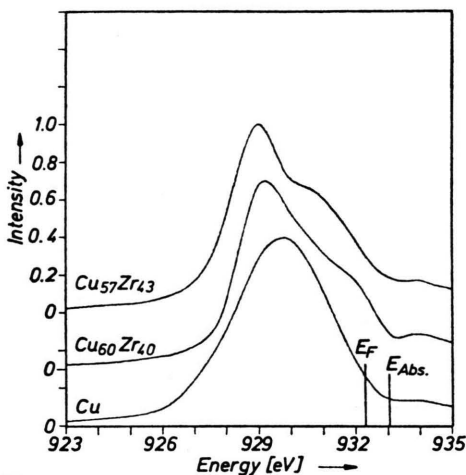
b)

Fig. 1. Lα — spectra of Cu in a) Crystalline intermetallic Cu-Zr-compounds, b) Amorphous Cu-Zr-alloys.

the spectra near the energy which corresponds to that of the absorption edge can be recognized. A shift of the maximum to higher energies with increasing Ti-concentration can also be stated. However, this shift is smaller than with Cu-Zr. At the high energy side with decreasing Cu-concentration a shoulder or a peak, respectively, is formed.

As mentioned above, the X-Ray-emission spectra can be interpreted in a certain way as a copy of the local partial density of states. Thereby the low energy part of the spectrum is formed by electrons from the lower band edge, the higher energy part in a corresponding way by electrons from the Fermi-edge. Thus follows, that the binding energy of the corresponding electrons becomes smaller with in-

creasing X-Ray energy. The position of the Fermi-energy can be determined by XPS-measurements of the next lower (L_{III}) electron states. For crystalline copper the value of the Fermi-energy is taken form [22] [2.6 eV $\triangleq$ distance of $(E_F - N_{max}(E))$]. The
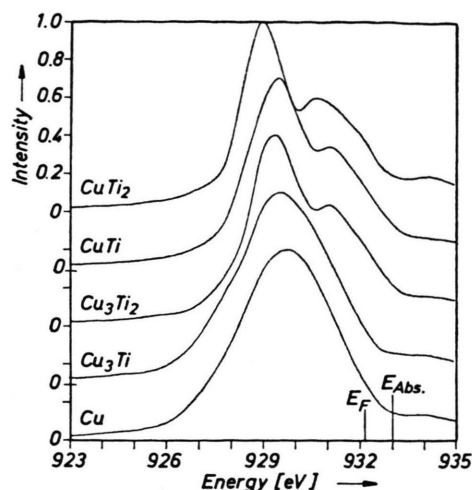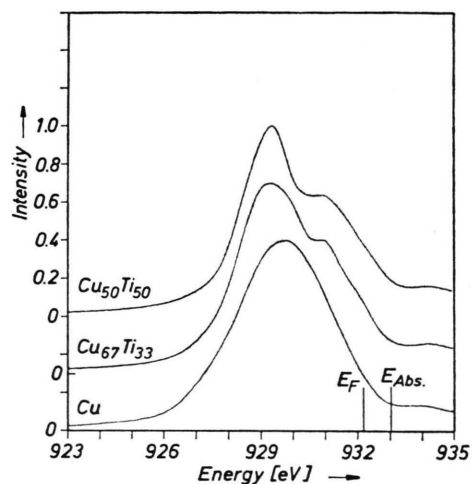

a)
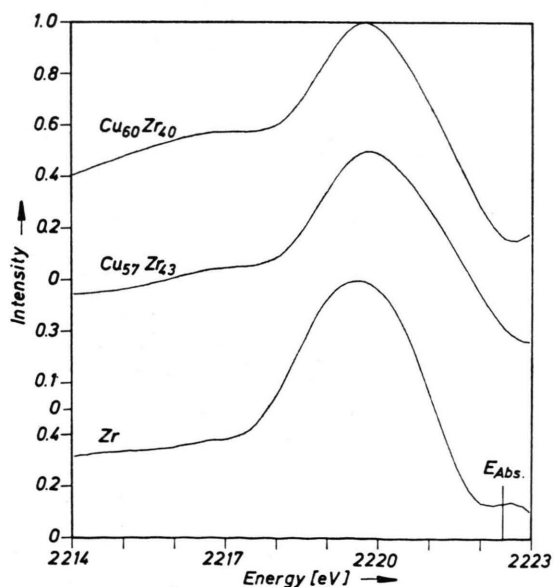
b)

Fig. 2. $L\beta$ — spectra of Zr in a) Crystalline intermetallic Cu-Zr-compounds, b) Amorphous Cu-Zr-alloys.

a)

b)

Fig. 3. $L\alpha$ — spectra of Cu in a) Crystalline intermetallic Cu-Ti-compounds, b) Amorphous Cu-Ti-alloys.

bump of the spectra in the region of the absorption edge is caused by the self absorption which is rather strong for these energies. This effect also can cause an asymmetry of the spectrum [13].

Self absorption effects could be avoided by using very small acceleration voltages. The instabilities of the electron optical system, however, would then become too large.

The shift of the Cu peak to lower energies can be interpreted as a shift of the maximum density of states to higher binding energies within the copper d-band. This means from the observation of the spectra of Zr, that the maximum density of states remains unchanged within the concentration range of the present work. There is only one exception,

namely with crystalline $Cu_{50}Zr_{50}$ since in this case the maximum of the Zr d-band lies at smaller binding energy.

The shift of the maximum with Cu-Ti specimens is smaller than that of Cu-Zr, which is in accordance to the UPS-experiments reported in [23]. The fact, that the shifts of the Cu-line are larger with Cu-Zr than with Cu-Ti are in agreement with the electronegativity difference which amounts to 0.5 in the first and to 0.3 in the latter case.

The shift of the maximum of density of states in Fig. 1a to smaller energies with rising Zr-concentration already was described in [15], [24] as well as the fact that the Zr-line remains nearly constant.

Finally it should be payed attention to the fact, that with increasing Zr- and Cu-concentration, respectively, a shoulder or a peak is formed at larger and smaller binding energies, respectively. This can be understood as a splitting up of the corresponding density of states which is in accordance with the calculated Cu- and Zr-density of states [5]. An electronic stabilization of the amorphous structure by compound formation, i.e. chemical short range order can be concluded from this result. Also by structural investigations a relatively strong chemical short range order in $Cu_{57}Zr_{43}$ as well as in $Cu_{66}Ti_{34}$ could be proved ([25], [26]).

### b) Systems Fe-B, Fe-P, Co-B, and Co-P

In Figs. 4a and 4b the spectra of the Fe-$L\alpha$-line in crystalline and amorphous Fe-B-alloys are shown. It follows from Fig. 4a, that the positions of the maxima of the spectra of the crystalline Fe-B-alloys are unshifted with exception of the alloy $Fe_{50}B_{50}$, where a shift of 0.3 eV to higher energies is observed.

The lines show a broadening with decreasing Fe-concentration. The spectra of the amorphous alloys show between $Fe_{86}B_{14}$ and $Fe_{80}B_{20}$ a decrease of the broadening at the low energy side. All amorphous Fe-B-alloys yield a larger intensity at the low energy side, which is much more pronounced in Fig. 5 with amorphous Fe-P. The increased intensity at the low energy side is in Fig. 5 (Fe-P) so strong that a shoulder is visible, whereas the remaining curve is in rather good accordance with crystalline Fe without additional line-broadening.

In Fig. 6 the Co-$L\alpha$-spectra of glassy $Co_{80}P_{20}$ and $Co_{81.5}B_{18.5}$ are compared with crystalline Co. The lines of $Co_{80}P_{20}$ and Co are nearly identical with small deviations at the left side. The spectrum of
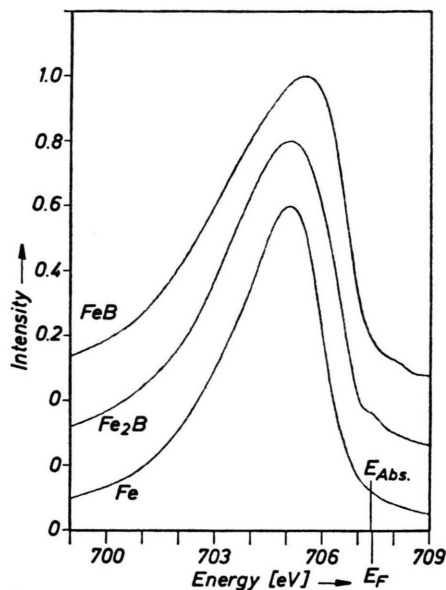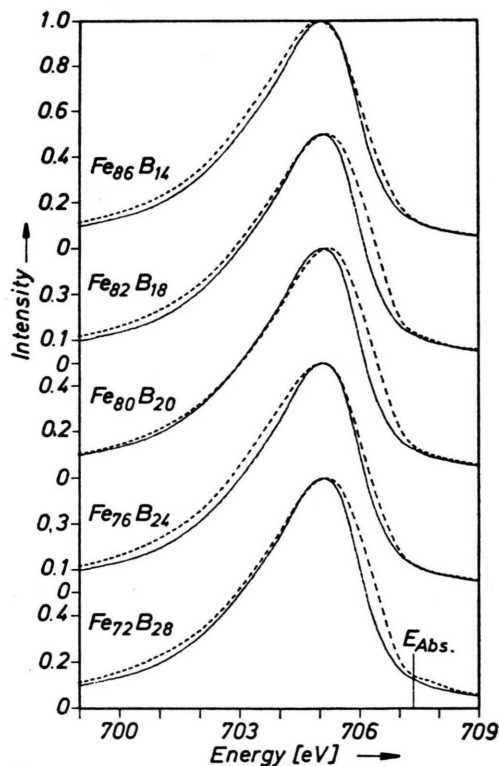
Fig. 4. $L\alpha$ — spectra of Fe in a) Crystalline Fe-B-alloys, b) Amorphous Fe-B-alloys (-----) and in crystalline Fe (——).
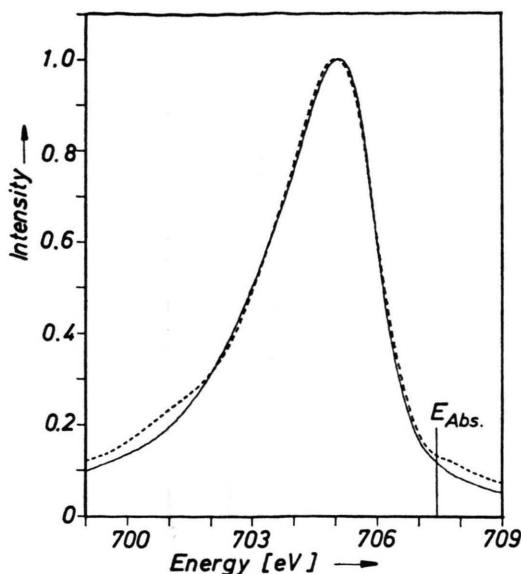
Fig. 5. Lα — spectra of Fe in amorphous $Fe_{80}P_{20}$ (-----) and in crystalline $Fe_{80}P_{20}$ (——).

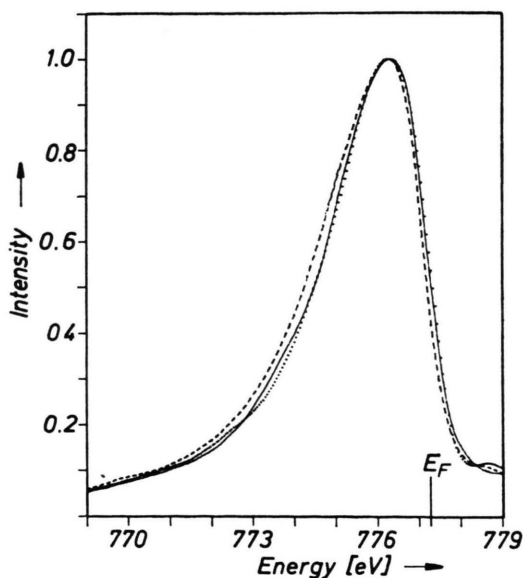Fig. 6. Lα — spectra of Co in amorphous $Co_{80}P_{20}$ (·····), amorphous $Co_{81.5}B_{18.5}$ (-----), crystalline Co (——).

$Co_{81.5}B_{18.5}$ shows a broadening at the low energy side.

Thus we can conclude from Fig. 4 to 6, that these specimens show nearly no changes in the X-Ray spectra and therefore in the corresponding density of states. The broadening of the Lα-line of the metallic glasses is also observed in the crystalline Fe-B-specimens.

The Fermi energy for pure iron is taken from [22]. The increased intensity at the low energy side of the line means increased density of states at higher binding energies. This result can be correlated for the Fe-metalloid-systems with the XPS-measurements of [27]. In that paper an additional XPS-peak could be observed which points on additional binding between B 2p- and Fe 3d-electrons. A shift of the peak to higher binding energy could not be recognized during the present work which is in contradiction to [27]. The additional binding by hybridization of 2p- and 3d-states is a hint on chemical short range order which stabilizes the amorphous structure. Also by diffraction experiments of metallic Fe-, Co-, and Ni-glasses a relatively strong chemical short range order could be found [7]. The similarity of the amorphous and the crystalline spectra signalizes a large similarity in the chemical short range order of the two phases.

These results are in agreement with the XPS-measurements of Ammamou and Krill [4]. However, Cartier [28] could not find a corresponding peak. In any case the prediction of a decrease of the density of states near the Fermi edge made by Nagel and Tauc theory [1], [2] cannot be confirmed by the present experiments.

c) Systems Fe-Si-B, Fe-Ge-P, and Mn-Si-P

In Fig. 7 the Lα-spectra of iron within the ternary amorphous phases $Fe_{76}Si_{18}B_6$, $Fe_{76}Si_{12}B_{12}$, and $Fe_{78}Ge_{12}P_{10}$ are shown. A shift of the lines in the direction to higher binding energies is clearly visible in the first two cases. The spectrum of Fe in $Fe_{78}Ge_{12}P_{10}$ corresponds in principle to that in $Fe_{80}P_{20}$ (see Figure 5). This means that apparently P can be replaced by Ge without changing the structure of the Fe d-band in the corresponding glass.

From Fig. 8 follows a good accordance of the Mn Lα-spectra of amorphous $Mn_{74}Si_{20}P_6$ and $Mn_{74}Si_{13}P_{13}$. In both cases they are shifted by 0.5 eV to the low energy side of the crystalline Mn. The shift of the maximum of the density of states in the Fe-Si-B-system shows an electronic stabilization of the glasses by lowering the energy. This means, as well as with Mn-Si-P, the existence of chemical short range order. This also was proven by diffraction experiments [8].

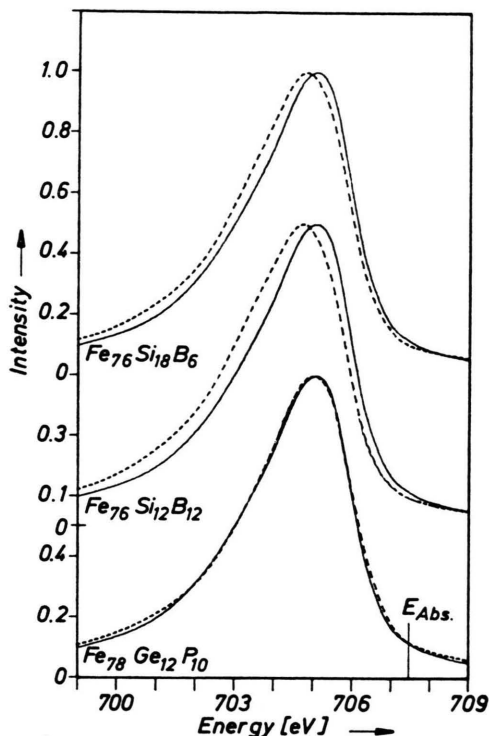Finally we can conclude that with the metallic glasses treated in the present paper always a shift

Fig. 7. Lα — spectra of Fe in amorphous $Fe_{76}Si_{18}B_6$, amorphous $Fe_{16}Si_{12}B_{12}$, amorphous $Fe_{78}Ge_{12}P_{10}$, in each case compared to crystalline Fe (——).
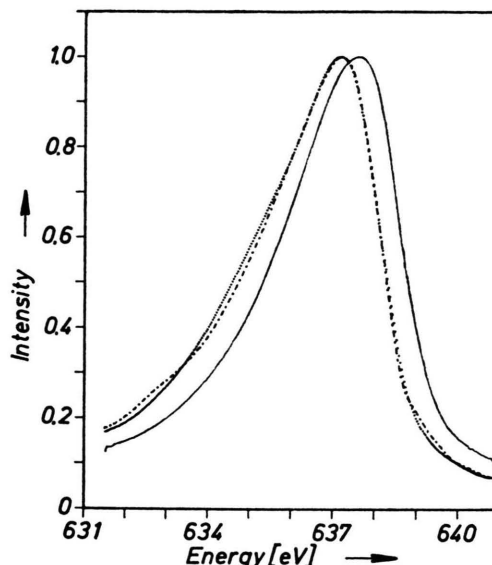
Fig. 8. Lα — spectra of Mn in amorphous $Mn_{74}Si_{20}P$ (·····), amorphous $Mn_{74}Si_{13}P_{13}$ (-·-·-·), crystalline Mn (——).

of the binding energy between the electrons and their corresponding atoms to higher binding energies can be observed as well as an agreement in the binding energy of the amorphous phase and the corresponding crystalline phase.

[1] S. R. Nagel and J. Tauc, Phys. Rev. Letters **35**, 380 (1975).
[2] S. R. Nagel, and J. Tauc, Inst. Phys. Conf. Ser. No. **30**, 283 (1977).
[3] J. Hafner, Phys. Review B **21**, 406 (1980).
[4] A. Ammamou and G. Krill, Solid-State Com. **33**, 1087 (1980).
[5] H. J. Güntherodt, P. Oelhafen, R. Lapka, H. U. Künzi, G. Indlekofer, J. Krieg, T. Laubscher, H. Rudin, U. Gubler, F. Rösel, K. P. Ackermann, B. Delley, M. Fischer, F. Greuter, E. Hauser, M. Liard, M. Müller, J. Kübler, K. H. Bennemann, and C. F. Hague, J. Physique C8, **41**, 381 (1980).
[6] F. Sommer, Z. Metallkde. **72**, 219 (1981).
[7] P. Lamparter, E. Nold, G. Rainer-Harbach, E. Grallath, and S. Steeb, Z. Naturforsch. **36a**, 165 (1981).
[8] G. Rainer-Harbach, P. Lamparter, and S. Steeb, Lecture at the DPG-Frühjahrstagung M129 (1981).
[9] G. Dräger in "Handbuch der Festkörperanalyse mit Elektronen, Ionen und Röntgenstrahlen"; O. Brümmer, J. Heydenreich, K. H. Krebs, and H. G. Schneider, Verlag Vieweg, Braunschweig 1980.
[10] H. Binder and E. Fluck in Mod. Phys. Chem.; E. Fluck and V. I. Goldanskii, Academic Press, London **2** (1979).
[11] P. J. Durham, D. Ghaleb, B. L. Györffy, C. F. Hague, J.-M. Mariot, G. M. Stocks, and W. M. Temmerman, J. Phys. F: Metal Phys. **9**, 1719 (1979).
[12] L. M. Watson in Band Structure Spectroscopy of Metals and Alloys, D. J. Fabian, and L. M. Watson, Academic Press, London 1973.

[13] C. Bonnelle, Ann. Phys. **1**, 439 (1966).
[14] H. Drack, Doctor-Thesis, TU Wien 1977.
[15] H. Drack, S. Kosina, and M. Grasserbauer, Fresenius Z. Anal. Chem. **295**, 30 (1979).
[16] A. Faessler, Angew. Chemie **83**, 51 (1972).
[17] M. A. Blochin, Methoden der Röntgenspektralanalyse, Verlag Otto Sagner, München 1964.
[18] S. Falch, Diplom-Thesis, University Stuttgart 1981.
[19] E. O. Brigham, The Fast Fourier Transform, Prentice-Hall, Inc., Englewood Cliffs, New Jersey 1974.
[20] W. Sperl, Diplom-Thesis, University Stuttgart 1980.
[21] J. A. Bearden, X-Ray Wavelength, Rev. Mod. Phys. **39**, 78 (1967).
[22] C. Bonnelle, in Soft X-Ray Band Spectra and the Electronic Structure of Metals and Materials, D. J. Fabian, Academic Press, London 1968.
[23] P. Oelhafen, E. Hauser, and H. J. Güntherodt, Sol. State Comm. **35**, 1017 (1980).
[24] P. Oelhafen, E. Hauser, and H. J. Güntherodt, Phys. Rev. Letters **43**, 15 (1979).
[25] P. Lamparter, G. Rainer-Harbach, and S. Steeb, ILL, Experimental Report Nr. 06-08-032 (15. 12. 1980).
[26] M. Sakata, N. Cowlam, and H. A. Davies, J. Phys. F: Metal. Phys. **9**, L 235 (1979).
[27] K. Suzuki, F. Itoh, M. Misawa, M. Matsura, T. Fukunaga, and K. Ikeno, Suppl. to Sci. Rep. RITU, **17**, 12 (1980).
[28] E. Cartier, Y. Baer, M. Liard, and H. J. Güntherodt, J. Phys. F: Metal Phys. **10**, 221 (1980).